Available online at www.sciencedirect.com
SCIENCE DIRECT®
Tectonophysics 381 (2004) 81–100
TECTONOPHYSICS
www.elsevier.com/locate/tecto

Structure of the lithosphere below the southern margin of the East European Craton (Ukraine and Russia) from gravity and seismic data

T.P. Yegorova[a,*], R.A. Stephenson[b], S.L. Kostyuchenko[c], E.P. Baranova[a], V.I. Starostenko[a], K.E. Popolitov[c]

[a] *Institute of Geophysics, National Academy of Sciences of Ukraine, Kiev, Ukraine*
[b] *Netherlands Research School of Sedimentary Geology, Vrije Universiteit, Amsterdam, The Netherlands*
[c] *GEON Centre, Ministry of Natural Resources of Russia, Moscow, Russia*

Received 25 March 2001; accepted 8 August 2002

Abstract

The present study was undertaken with the objective of deriving constraints from available geological and geophysical data for understanding the tectonic setting and processes controlling the evolution of the southern margin of the East European Craton (EEC). The study area includes the inverted southernmost part of the intracratonic Dnieper-Donets Basin (DDB)–Donbas Foldbelt (DF), its southeastern prolongation along the margin of the EEC–the sedimentary succession of the Karpinsky Swell (KS), the southwestern part of the Peri-Caspian Basin (PCB), and the Scythian Plate (SP). These structures are adjacent to a zone, along which the crust was reworked and/or accreted to the EEC since the late Palaeozoic. In the Bouguer gravity field, the southern margin of the EEC is marked by an arc of gravity highs, correlating with uplifted Palaeozoic rocks covered by thin Mesozoic and younger sediments. A three-dimensional (3D) gravity analysis has been carried out to investigate further the crustal structure of this area. The sedimentary succession has been modelled as two heterogeneous layers—Mesozoic–Cenozoic and Palaeozoic—in the analysis. The base of the sedimentary succession (top of the crystalline Precambrian basement) lies at a depth up to 22 km in the PCB and DF–KS areas. The residual gravity field, obtained by subtracting the gravitational effect of the sedimentary succession from the observed gravity field, reveals a distinct elongate zone of positive anomalies along the axis of the DF–KS with amplitudes of 100–140 mGal and an anomaly of 180 mGal in the PCB. These anomalies are interpreted to reflect a heterogeneous lithosphere structure below the supracrustal, sedimentary layers: i.e., Moho topography and/or the existence of high-density material in the crystalline crust and uppermost mantle. Previously published data support the existence of a high-density body in the crystalline crust along the DDB axis, including the DF, caused by an intrusion of mafic and ultramafic rocks during Late Palaeozoic rifting. A reinterpretation of existing Deep Seismic Sounding (DSS) data on a profile crossing the central KS suggests that the nature of a high-velocity/density layer in the lower crust (crust–mantle transition zone) is not the same as that of below the DF. Rather than being a prolongation of the DDB–DF intracratonic rift zone, the present analysis suggests that the KS comprises, at least in part, an accretionary zone between the EEC and the SP formed after the Palaeozoic.

Keywords: Donbas Foldbelt; Karpinsky Swell; 3D gravity modelling; Deep seismic sounding (DSS); Crust–mantle structure

* Corresponding author.
E-mail address: egorova@igph.kiev.ua (T.P. Yegorova).

0040-1951/$ - see front matter © 2004 Elsevier B.V. All rights reserved.
doi:10.1016/j.tecto.2002.08.003

1. Introduction

A key point in studying the East European Craton (EEC) is understanding the tectonic setting and processes controlling the evolution of its margins. The southern margin, along which the crustal segments were reworked and/or accreted in late Palaeozoic–Triassic times (Nikishin et al., 1996), is of the same importance as the western margin of the EEC marked by Trans-European Suture Zone (TESZ). However, in contrast with the TESZ, crossed by numerous seismic profiles (cf. Thybo et al., 1999), the deeper structure of the southern margin of the EEC is poorly investigated, and little is known definitively about the geodynamic processes that controlled its evolution.

The key object of this study is the Donbas Foldbelt (DF)–Karpinsky Swell (KS) region (Fig. 1), lying at the junction of the Precambrian EEC, the Scythian Plate (SP), and the intracratonic Dnieper-Donets Rift Basin (DDB). Among the deepest sedimentary basins of the European continent, the Karpinsky Swell (KS) and the Peri-Caspian Basin (PCB) are situated along the southern margin of the EEC and have sedimentary successions greater than 20 km. Although the role of intracratonic rifting in forming the DDB and its inverted southeasternmost part—the Donbas Foldbelt (DF)—is established (e.g., Stephenson et al., 2001), the nature and processes governing the development of the KS that lies directly to the southeast of the DF (Fig. 1) are poorly understood. Is the sedimentary succession of the KS a prolongation of the intracratonic DDB–DF rift basin, in which case, the southern margin of the EEC can be considered as rift originated? Or does its formation relate more to

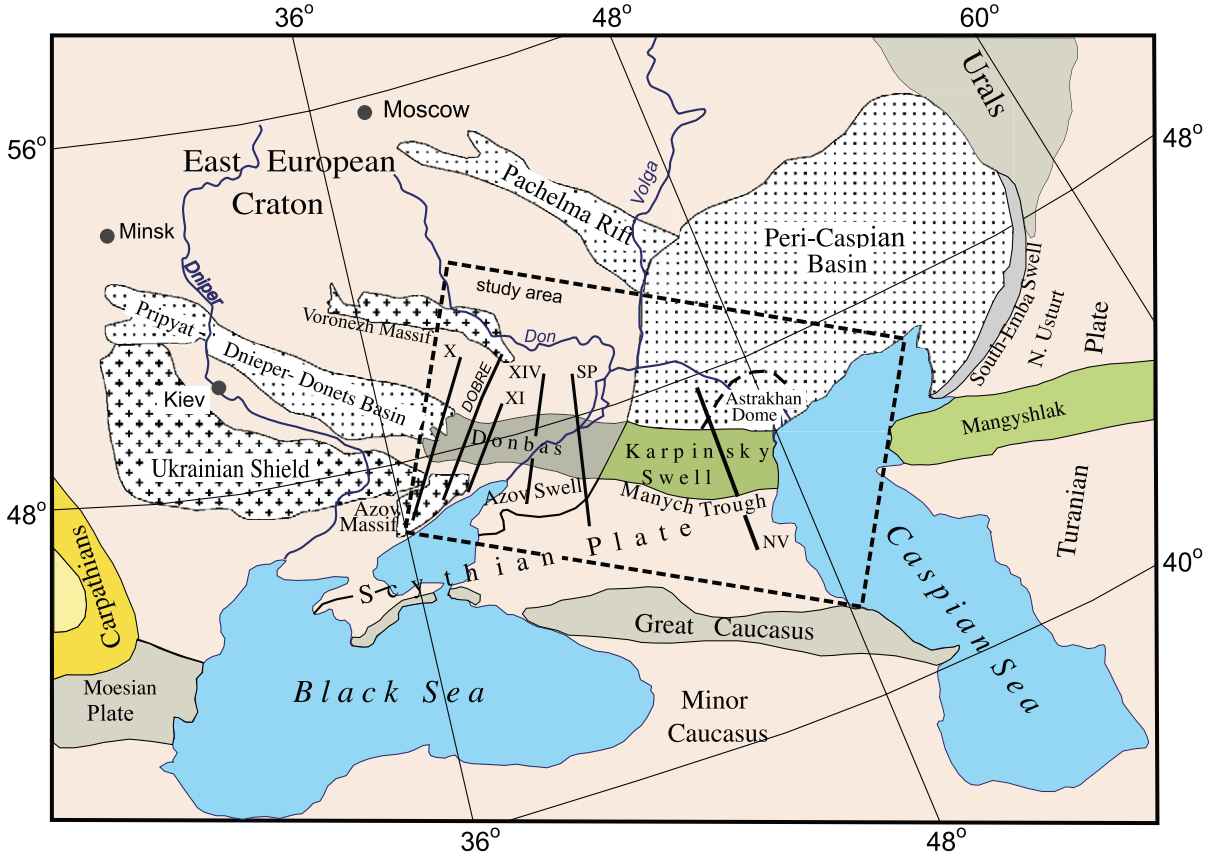

Fig. 1. Main tectonic elements of the southern part of the East European Craton and Caucasus region. The dashed rectangle shows the region of the 3D gravity analysis and modelling study. Solid lines indicate DSS profiles in the Donbas Foldbelt–Karpinsky Swell region; the thicker line labelled NV is the Nakhichevan–Volgograd DSS profile.

processes involved in the suturing of the SP to the EEC in late Palaeozoic–Mesozoic times?

The present study is aimed at deriving constraints from available geological and geophysical data on lithospheric structure below the DF–KS region and adjoining units to allow better tectonic reconstructions of the southern EEC margin. This is carried out by a regional 3D gravity modelling study, including gravity "backstripping". In this method, residual gravity anomalies obtained by subtracting the modelled effects of the supracrustal (sedimentary) succession from the observed field are interpreted to be caused by density heterogeneities in the underlying lithosphere. For example, a high-density body, correlated with a zone of high seismic velocities in the middle–lower crust, was revealed in a similar study below the southeastern part of the DDB and the DF, and interpreted as basic and ultrabasic material intruded into the crystalline crust during Late Palaeozoic rifting (Yegorova et al., 1999). This study can be considered as a continuation of the study by Yegorova et al. (1999), southeastwards to the KS area, although it also presents a reinterpretation of existing Deep Seismic Sounding (DSS) data along a profile crossing the KS (Nakhichevan–Volgograd).

2. Geological setting

The Donbas Foldbelt (DF) and the Karpinsky Swell (KS) are contiguous parts of a system of elongated sedimentary basins about 100–120 km in width, located on the southern margin of the EEC. It divides the Scythian Plate (SP) in the south from Voronezh Massif and Peri-Caspian Basin (PCB) in the north (Fig. 1). The DF and the KS have been generally thought to be cogenetic segments of the DDB system. Karpinskii (1883) proposed that they formed part of a lineament running from Poland (Keletsko-Sandomir Swell) through the Pripyat Trough in Belarus, the DDB–DF–KS, east across the Caspian Sea, and thence through to the Turanian plate in Asia (Mangyshlak Karatau). This tectonic zone was named the Sarmato–Turanian lineament by Aizberg et al. (1971).

Recent investigations have shown convincingly that the DDB and the DF, as well as the PCB, were formed mainly as a result of Middle–Late Devonian rifting (e.g., Stovba et al., 1996; Brunet et al., 1999), accompanied by voluminous magmatism activity possibly under the influence of hot spot activity (Kusznir et al., 1996; Wilson and Lyashkevich, 1996).

Postrift basin subsidence and thick sediment accumulation continued during the Carboniferous and later, especially in the southeastern Donets segment of the rift, where thick strata (about 15 km in thickness) of Carboniferous coal-bearing continental deposits were accumulated. The total thickness of the sedimentary succession in the DF reaches more than 20 km (Chekunov et al., 1992; Stovba and Stephenson, 1999). The Azov–Rostov segment of the Ukrainian Shield (the Azov Massif and Azov Swell in Fig. 1) probably was a source of clastic material for sediment accumulation in the DF (Khain, 1977).

The Urals Orogeny occurred in Early Permian, and this affected the eastern and southeastern margins of the EEC, leading to the isolation of the PCB at that time and to its filling by thick Kungurian evaporites, as the continental Usturt Massif moved up from the south and the South Emba Swell developed (Zonenshain et al., 1990). The PCB is characterised by its enormous size (0.5×10^9 km^2), by a very thick sedimentary succession (reaching 20 km in the basin centre including up to 4 km of salt-bearing rocks) directly overlying a thinned crust apparently devoid of any "granitic" layer (cf. Brunet et al., 1999). The affinity of crust beneath the PCB—whether it is oceanic (Zonenshain et al., 1990) or thinned continental (Belousov, 1990)—has been a matter of dispute for many years.

It has been conventionally thought that the inversion of the DF–KS segment of the DDB was related to the evolution of the Scythian Orogen (Milanovsky, 1987, 1992) during the Early Permian (contemporaneous with the Urals Orogeny). However, Stovba and Stephenson (1999) demonstrated that Latest Carboniferous–Early Permian tectonic reactivations in the DDB and DF occurred in a transtensional stress regime stretching, while the main phases of compressional tectonics forming the DF were Cimmerian (Latest Triassic–Earliest Jurassic) and, especially, Alpine (Latest Cretaceous–Earliest Tertiary). New paleostress analyses of the DF and environs support this interpretation (Saintot et al., 2003). Similar phases of compressional deformations are established for the KS (Sobornov, 1995).

In the Late Triassic, the southern margin of the EEC came under the influence of convergence in the vicinity of the Caucasus/Scythian Plate, accompanied by further deformations in the KS (Nikishin et al., 1996). In contrast with the DF, where Carboniferous coal-bearing continental deposits are exposed at the surface, Palaeozoic rocks on the KS are covered by Mesozoic–Cainozoic sediments of up to 2 km in thickness, formed in shallow-marine conditions (e.g., marine shales). Folds and other compressional structures easily seen in the DF cannot be confidently mapped in the KS; the Jurassic sedimentary cover becomes more even widespread and increases in thickness.

3. Geophysical data

The gravity field on the southern margin of the EEC is characterised by a zone of increased Bouguer anomalies (Yegorova et al., 1995) and isostatic anomalies (Artemjev, 1975). A band of positive anomalies with magnitude 20–35 mGal over the DF and the KS can be seen in Fig. 2, consistent with the Carboniferous coal-rich shales exposed in the DF and with the uplifted, folded Palaeozoic basement of the KS, the latter covered by thin Mesozoic–Cainozoic sediments. Further to the east, this band passes into an area of positive (up to 35 mGal) Bouguer anomalies over the northern part of the Caspian Sea and, changing direction to the northeast, continues to the Urals. Over the northern part of the Caspian Sea and Southern Urals, it coincides with an area of anomalous magnetic field character (Fig. 3).

The magnetic field of the DF is negative and subdued in the central part of the basin against a background of more intense anomalies over the Azov Massif of the Ukrainian Shield and, especially, the Voronezh Massif, famous for the Kursk magnetic

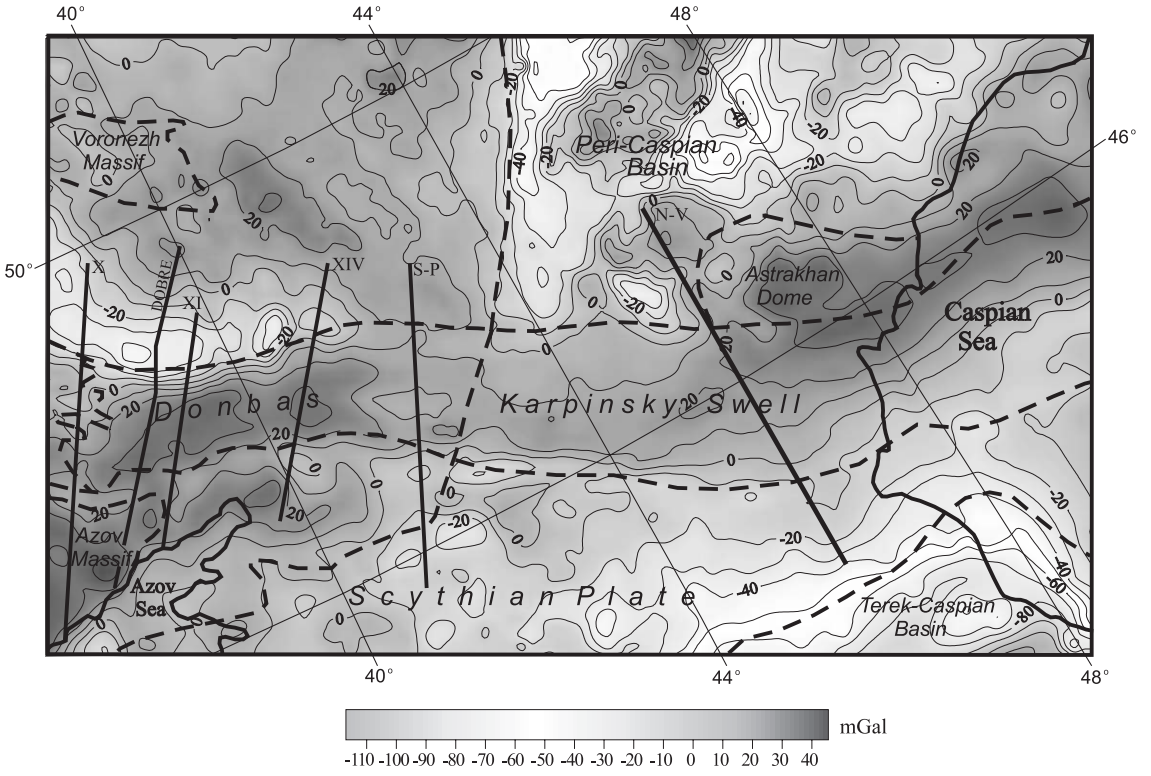

Fig. 2. Map of the observed gravity field (Bouguer anomalies averaged on a 10 km grid) for the southern part of the East European Craton and Fore–Caucasus region, the area within the rectangle in Fig. 1. Contour interval is 10 mGal. Dashed lines outline tectonic units; solid lines indicate DSS profiles.

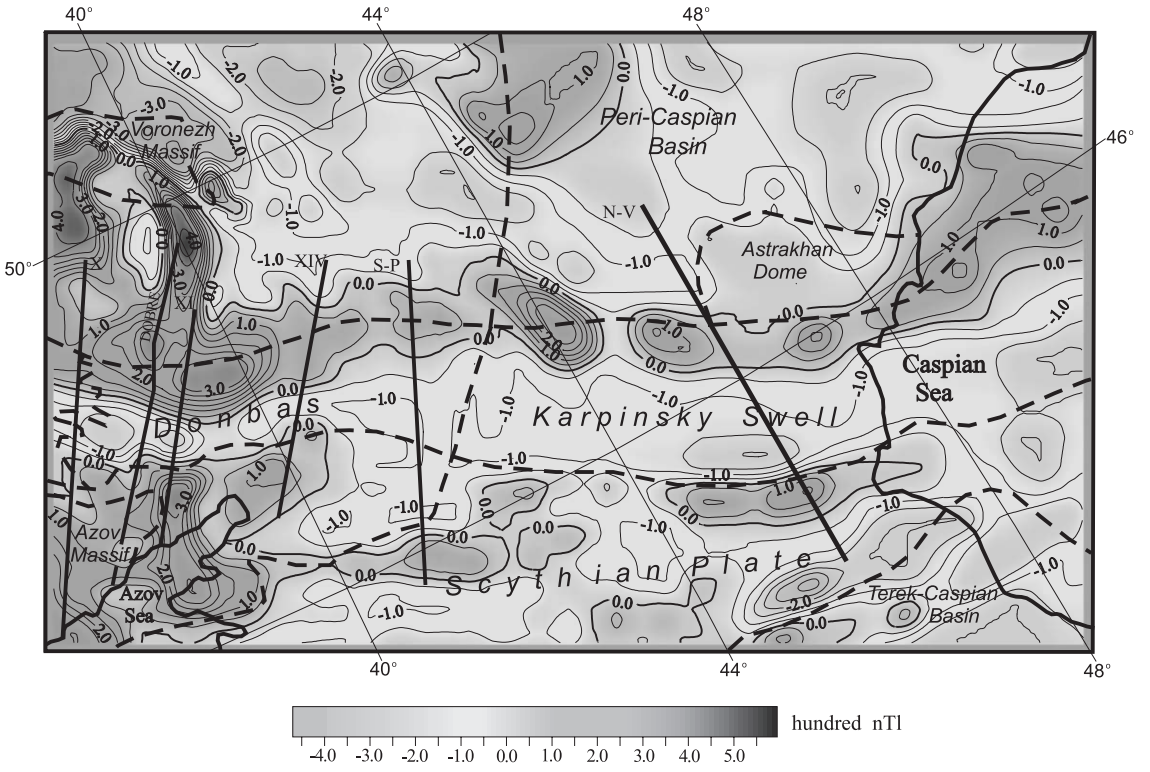

Fig. 3. Map of anomalous magnetic field for the southern part of the East European Craton and Fore–Caucasus region, the area within the rectangle in Fig. 1 (from Simonenko and Pashkevich, 1990). Contour interval is 50 nTl. Dashed lines outline tectonic units; solid lines indicate DSS profiles.

anomaly related to iron deposits (Dobrohotov, 1961; Kutas and Pashkevich, 2000). A similar negative magnetic field also characterises the KS. Along the northern and southern border zones of the KS, a series of linear magnetic anomalies are seen (Fig. 3). In particular, magnetic field heterogeneity characterises the southern flank of the KS, where they can be related to basic magmas intruded in a junction zone of the Manych Trough with the KS (Nazarevich et al., 1986).

The mosaic gravity field pattern of the PCB seen in Fig. 2 is composed of linear and rectangular gravity lows, caused by the presence of salt, and highs (two of which—Aralsor and Emba—are located within the limits of the study area) which are associated with the presence of high-density (mafic) thinned crystalline crust (Volozh et al., 1975; Brunet et al., 1999).

Seismic investigations (DSS and some reflection seismic) were carried out in the area of the DF–KS transition from the 1960s to the 1980s along a number of profiles shown in Fig. 1 (and subsequent figures). These include the Nakhichevan–Volgograd (Krasnopevtseva, 1984), Surovikino–Peschanokopskaya (Konovaltcev, 1978; Yurov, unpublished data), and Bataisk–Milutinskaya (labelled XIV in the figures; Borodulin, 1973) profiles as well as profiles X (Nogaisk–Svatovo) and XI (Novoazovsk–Titovka) published in Ilchenko (1996) and Ilchenko and Stepanenko (1998). As a result of these studies, the configuration of the basins, the structure of the sedimentary cover, and the main features of the structure of the underlying crystalline crust have been fairly well determined. P-wave velocities in the sedimentary succession reach values up to 5.8 kms^{-1} (compared with 6.0 kms^{-1} and higher in the basement), and the top of the crystalline basement lies at the depth of 16–20 km. In the lower crust below the DF, two main boundaries, interpreted together as a double Moho

(Pavlenkova, 1995) or as the upper and lower boundaries of a "crust–mantle mixture" (Ilchenko, 1996; Ilchenko and Stepanenko, 1998), were identified. Refracted seismic phases were not recorded from this layer and, as such, a confident determination of which of these boundaries represented the Moho was not possible. (More recent refraction/wide-angle seismics places the Moho at a roughly constant depth of about 40 km beneath the DF; DOBREfraction'99 Working Group, 2003). In the lower crust below the KS, several reflectors have been distinguished as well as a refracting interface with upper mantle velocities (Krasnopevtseva, 1984).

4. Three-dimensional gravity analysis: method and results

4.1. Methodology used in the 3D gravity analysis

The three-dimensional (3D) gravity analysis utilises a "backstripping" technique, whereby the calculated effect of model layers, whose structure and properties are constrained by independent data, are successively removed from the observed gravity field. Previous investigations (Yegorova et al., 1999; Yegorova, 2000) have demonstrated that backstripping is a suitable method to apply to regions where lithospheric structure is hidden under a great thickness of sediments. Calculated residual anomalies (observed anomalies less the effect of the backstripped layers) can be interpreted as being due to density heterogeneties in the underlying layers (although "errors" in parameterising the backstripped layers cannot be excluded).

To calculate the gravity effect of backstripped layers, "anomalous" densities $\Delta\rho$ are calculated in reference to an average value of 2820 kgm^{-3} for the crystalline crust. The determination of this value is based on observations for Precambrian cratonic crust by Kozlenko (1986) and was used in previous studies of the DDB and DF (Yegorova et al., 1999; Yegorova, 2000). It is similar to the estimates made by Christensen and Mooney (1995) and by Gordienko (1999).

The 3D gravity analysis has been carried out using an automated system intended for modelling the layered media represented by a set of a maps (cf. Starostenko et al., 1997). The kernel of the system is the algorithm for solving the direct gravity problem for differently approximated elementary bodies with a complex distribution of density with depth (Starostenko and Legostaeva, 1998).

4.2. Supracrustal structural model

The objective of the present study is to elucidate in lithospheric heterogeneities caused, for example, by Moho topography and/or the occurrence of density anomalies in the consolidated crust and/or in the uppermost mantle. The residual gravity effect of such heterogeneities can reach some hundreds of mGal (Artemjev et al., 1994; Yegorova et al., 1998). Accordingly, the initial supracrustal structural model, to be used in the subsequent quantitative gravity analysis, consists of two layers (Fig. 4): Mesozoic–Cainozoic-aged low-density sediments and a higher density layer of highly compacted Palaeozoic sediments, including folded basement, overlying crystalline Palaeozoic and Precambrian basement.

Fig. 4a shows the depth to the base of the first of these; in the PCB, this layer includes Kungurian (Permian) salt as well as the postsalt deposits (as bounded by the "under-salt" seismic horizon P1; Brunet et al., 1999). This layer is very thin in the vicinity of the KS (1–2 km) and is effectively absent in the DF in contrast with the significant thickness of up to 9 km in the PCB and Terek-Caspian Basin (TCB). On the SP, the Stavropol High is distinguished by an uplift of the Palaeozoic basement to a depth of 1.6 km.

Fig. 4b shows the top of crystalline basement, hence the base of the second supracrustal layer. The DF–KS trend is characterised by an intense deepening of the base of Palaeozoic rocks, filling a narrow NW–SE trough with a maximum depth of more than 20 km in the DF. This joins a sharp linear NE–SW trough as deep as 18 km in the PCB corresponding to the Central Peri-Caspian Depression. The uplift of the top of the Palaeozoic supracrustal layer mirrored by the extreme deepening of its base (top of Precambrian basement) in the DF–KS area is illustrated in three dimensions in Fig. 5.

The maps shown in Fig. 4 are based on data prepared initially at a scale of 1:1,000,000 and have been gridded for purposes of the 3D modelling by taking data averages over 10×10 km cells. The grids

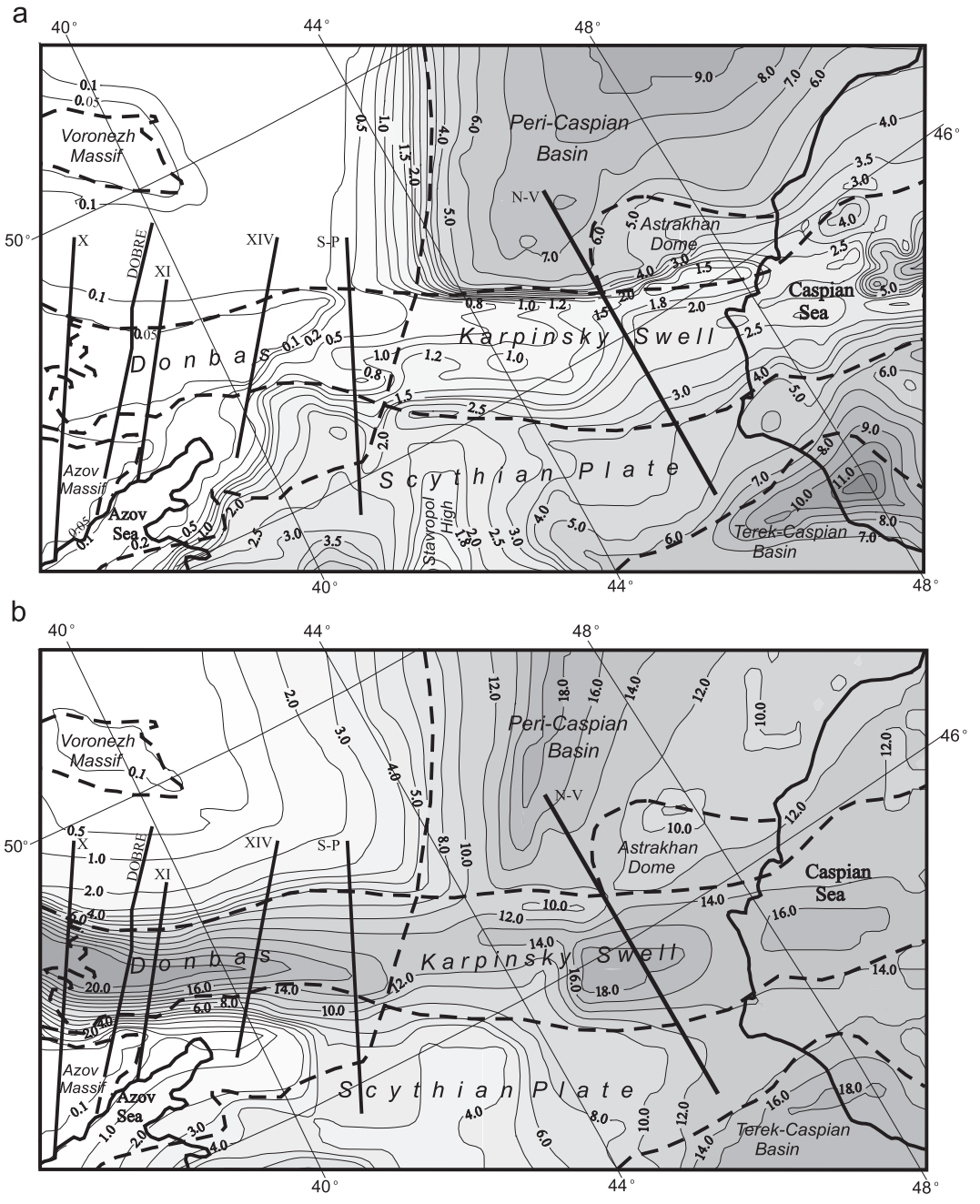

Fig. 4. (a) Depth (km) to the bottom of the upper sedimentary layer (supracrustal layer 1) consisting of low-density Mesozoic–Cainozoic sediments (above Palaeozoic sedimentary layer rocks), constructed using data from the GEON Centre and "Spetsgeofizika" of Russian Ministry of Natural Resources, as well as data from Muratov (1975) for the depth of Palaeozoic basement of the SP and Bogdanov and Khain (1981) in the Fore–Caucasus region. (b) Depth (km) to the bottom of the lower sedimentary layer (supracrustal layer 2) consisting of compacted Palaeozoic sediments and folded basement (above crystalline basement), based mainly on unpublished GEON data, complemented for the DF by the Atlas of Geological Structure and Oil and Gas Resources of the Dnieper-Donets Basin (1984) and taking into account Bogdanov and Khain (1981). Dashed lines outline tectonic units; solid lines indicate DSS profiles mentioned in the text.

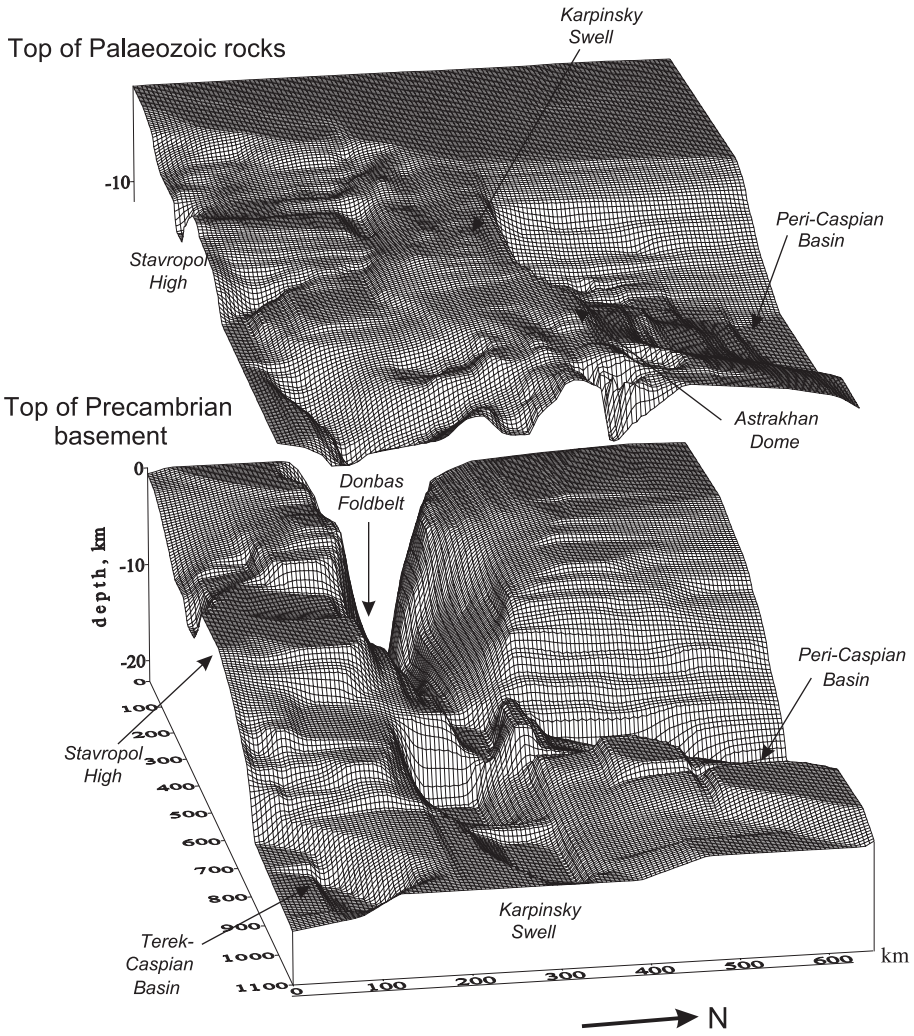

Fig. 5. 3D plot of the model used in present gravity backstripping analysis. The upper surface shows the top of Palaeozoic rocks (Fig. 4a) and the lower surface shows the top of Precambrian crystalline basement (Fig. 4b).

themselves cover a larger area than those shown by 200 km in every direction in order to alleviate gravitational edge effects. The width of the extrapolated zone, being 10 times the maximum depth of the model (20 km) is considered to be more than adequate.

4.3. Densities

Layer densities were derived from laboratory measurements on rocks from the study area (Ozerskaya and Podoba, 1967) and borehole observations for appropriate rock types and geological setting. Fig. 6a shows the average density adopted for supracrustal layer 1 (Mesozoic–Cainozoic sediments). In the SP, this layer is represented mainly by sandy-argillaceous deposits with density of about 2300 kgm^{-3}. The highest average densities for this layer (up to 2600 kgm^{-3}) are those of the metasediments of the central part of the TCB, where the layer thickness is more than 10 km (Fig. 4a). An essential consideration for gravity modelling in the present study area is an appropriate choice of average density for this layer in the PCB where Kungurian salt-bearing deposits comprise half

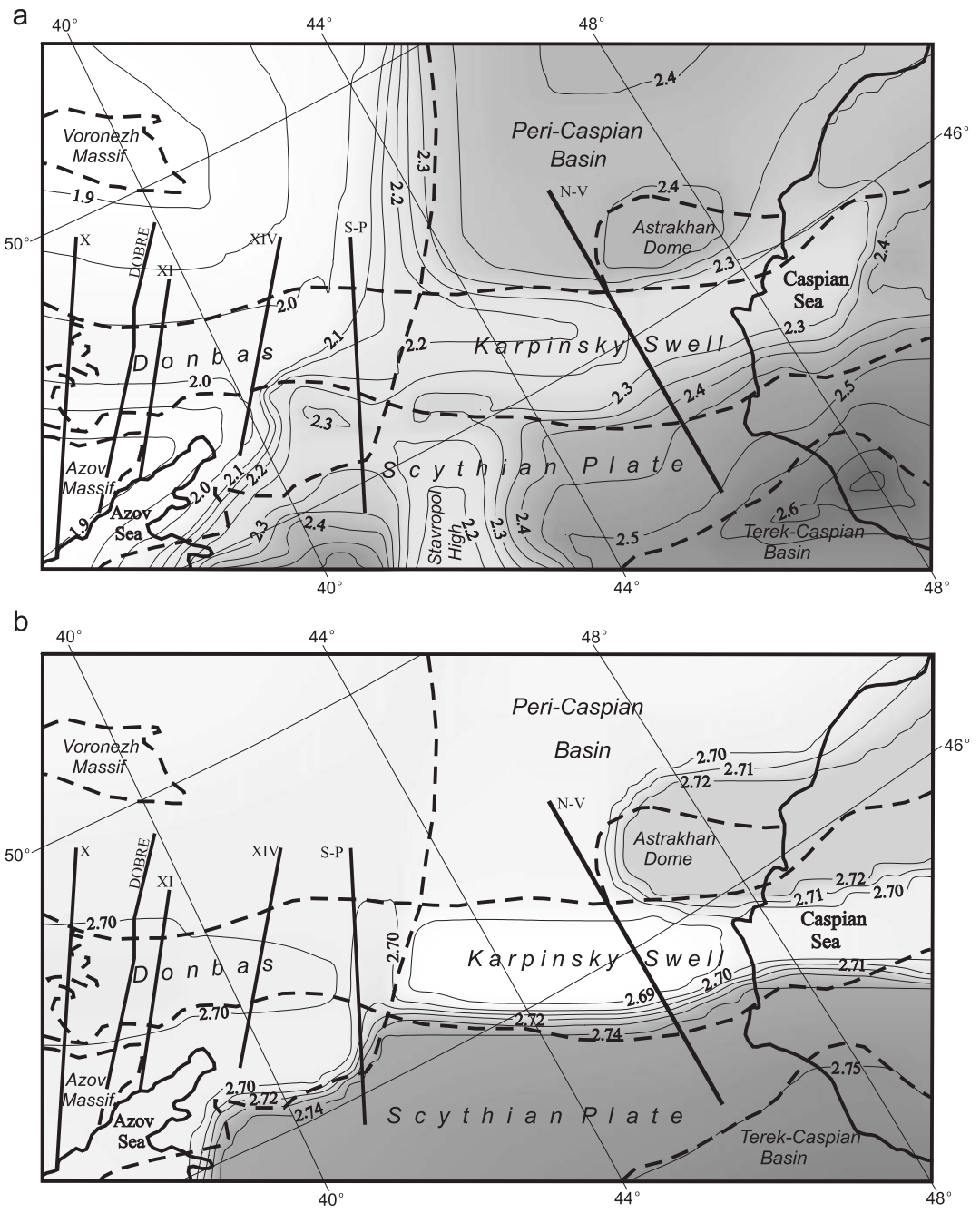

Fig. 6. Distribution of average density (10^{-3} kgm^{-3}) of the two model layers defined in Fig. 4: (a) the upper layer of Mesozoic–Cainozoic sediments; (b) the lower layer of Palaeozoic rocks (compacted sediments and folded basement). Dashed lines outline tectonic units; solid lines indicate DSS profiles.

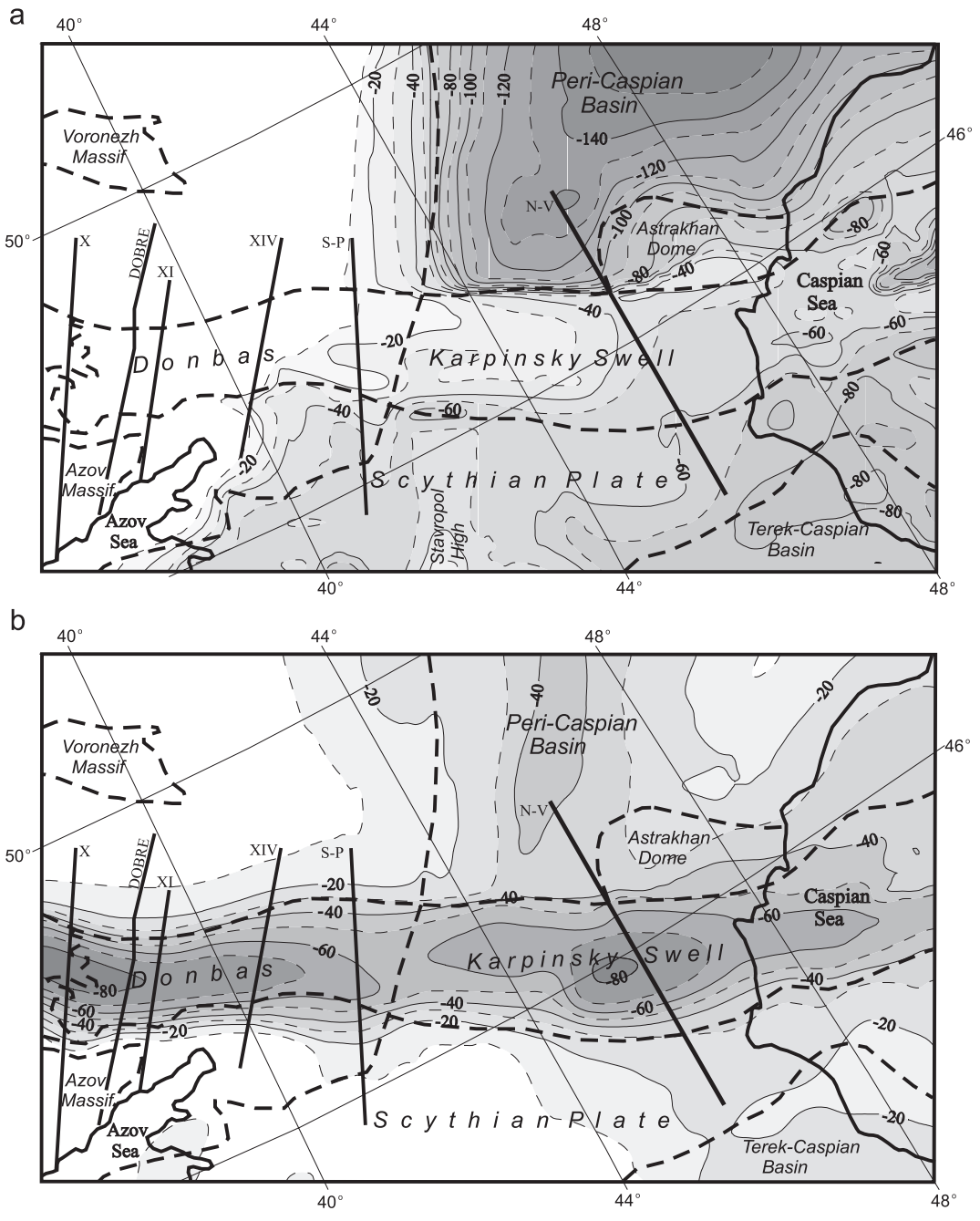

Fig. 7. Gravity effect (mGal) of the two model layers confined by interfaces shown in Fig. 4 and densities shown in Fig. 6: (a) the upper layer of Mesozoic–Cainozoic sediments; (b) the lower layer of Palaeozoic rocks. Main contour interval is 20 mGal. Dashed lines outline tectonic units; solid lines indicate DSS profiles.

of its thickness. Densities of these deposits lie in the range 2170–2200 kgm^{-3} and, for the layer as whole, in the range 2180–2550 kgm^{-3} (Nevolin and Kunin, 1977). An average interval density varying from 2300–2350 kgm^{-3} at the southern flank of the PCB to 2400 kgm^{-3} in the basin centre (northern edge of Fig. 6a) has been adopted.

Fig. 6b shows the adopted average density in the lower supracrustal layer of Palaeozoic rocks (including folded basement and consolidated sediments) taken from Ozerskaya and Podoba (1967). The Palaeozoic basement of the SP, thought to comprise mainly of Devonian–early Carboniferous clastic sediments that are intensively folded and affected by low-grade metamorphism, displays a slightly higher average density than elsewhere (2740 kgm^{-3}). The average densities of Palaeozoic rocks of the DF and the KS were assumed to be roughly the same (2690–2700 kgm^{-3}) based on borehole samples and geological data (Ozerskaya and Podoba, 1967; Golizdra and Popovich, 1998). In the DF, this layer is exposed at the surface and consists of mildly deformed Late Devonian and Carboniferous strata—including some magmatic rocks and significant coal deposits—developed in a rift basin and subsequently uplifted (e.g., Stovba and Stephenson, 1999; McCann et al., 2003). In the KS, in contrast to the DF, this layer is mainly composed of monotonous grey argillite strata of Carboniferous and Early Permian age without significant folding or magmatism. A zone of denser Palaeozoic rocks (up to 2730 kgm^{-3}) in the southern part of the PCB is related to more highly compacted and altered sedimentary rocks in the vicinity of the Astrakhan Dome (Ozerskaya and Podoba, 1967).

4.4. Gravity calculations

The gravity effects of the two supracrustal layers, calculated with respect to the reference density 2820 kgm^{-3} mentioned above, are shown in Fig. 7. These maps naturally correlate closely with the structure maps on which they are based, as shown in Fig. 4. The gravity effect of the first layer (Fig. 7a) is smallest where Palaeozoic basement is uplifted and shallowest (the DF and KS) and more significant in areas of thicker low-density sedimentary cover, such as the

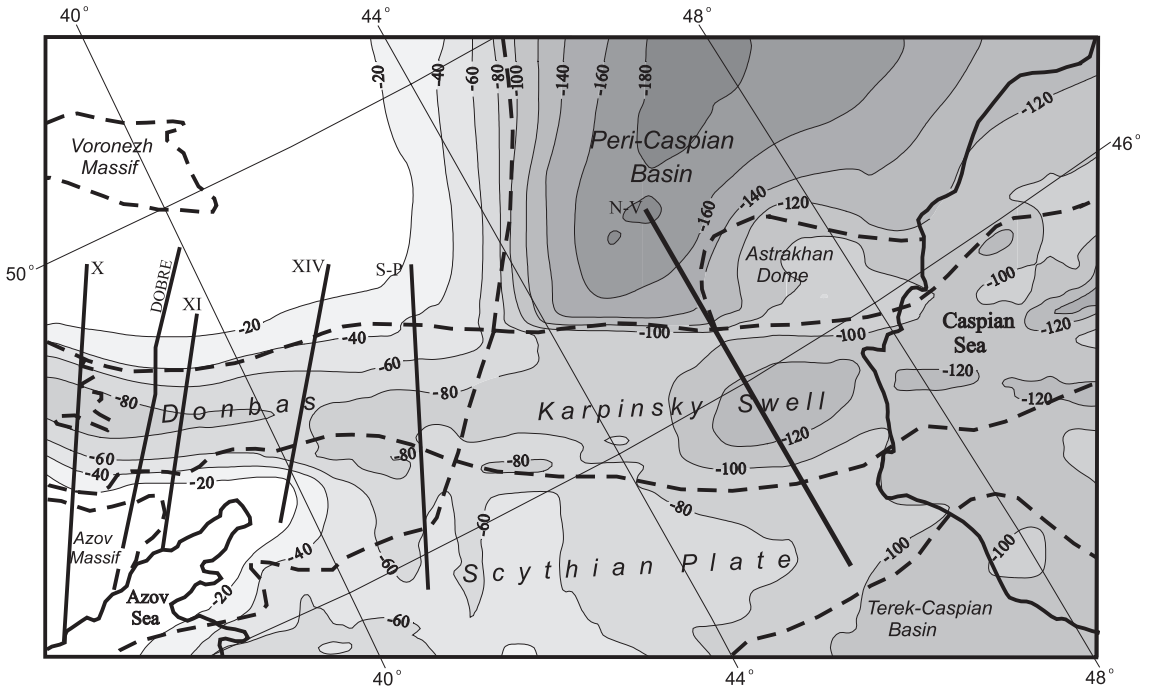

Fig. 8. Total gravity effect of the two supracrustal model layers (mgal). Contour interval is 20 mGal. Dashed lines outline tectonic units; solid lines indicate DSS profiles.

PCB, where it reaches −150 mGal, and the SP and TCB (−60 to −80 mGal). The gravity effect of the lower layer (Fig. 7b) is greatest along the DF–KS axis (−60 to −80 mGal) and in the central PCB (< −40 mGal), where the layer is thickest. Fig. 8 shows the combined effect of both layers. It is greatest in the PCB (< −180 mGal).

The residual gravity field, which can be assumed to be mainly due to sources beneath the defined supracrustal layers, is obtained by subtracting the effect of these layers (Fig. 8) from the observed Bouguer gravity field (Fig. 2), as shown in Fig. 9. Positive residual anomalies in the range 80–140 mGal lie along the DF–KS axis. A series of positive anomalies in the PCB (160–180 mGal) correlates with the total thickness of sediments in the basin and with local gravity highs seen in the observed field. Obviously, these results depend not only on the structural supracrustal model but also on the assigned densities for these. In particular, the inferred residual positive strip along the DF–KS is significant in the framework of the ensuing tectonic interpretations. Accordingly, a number of tests were carried out in which limiting densities for supracrustal layer 2 (the main model element controlling the residual gravity field) were adopted. These tests demonstrated that, although the magnitudes of the residual anomalies changed, the basic pattern of residual anomalies seen in Fig. 9 along the DF–KS axis is qualitatively a robust feature of the residual gravity field.

5. Two-dimensional model of crustal structure across the Karpinsky Swell–Scythian Plate

5.1. Reinterpreted Nakhichevan–Volgograd DSS data

The N–S orientated Nakhichevan–Volgograd DSS profile (labelled N–V on Fig. 1 and subsequent figures) is nearly 800 km long and crosses the Minor and Greater Caucasus to the south with a northern termination in the PCB in the vicinity of Volgograd. It was acquired in 1964 by the "Spetsgeofizika" of the Ministry of Geology of the former Soviet Union. Baranova and Pavlenkova (2003) have recently reinterpreted these data along the northern 430 km seg-

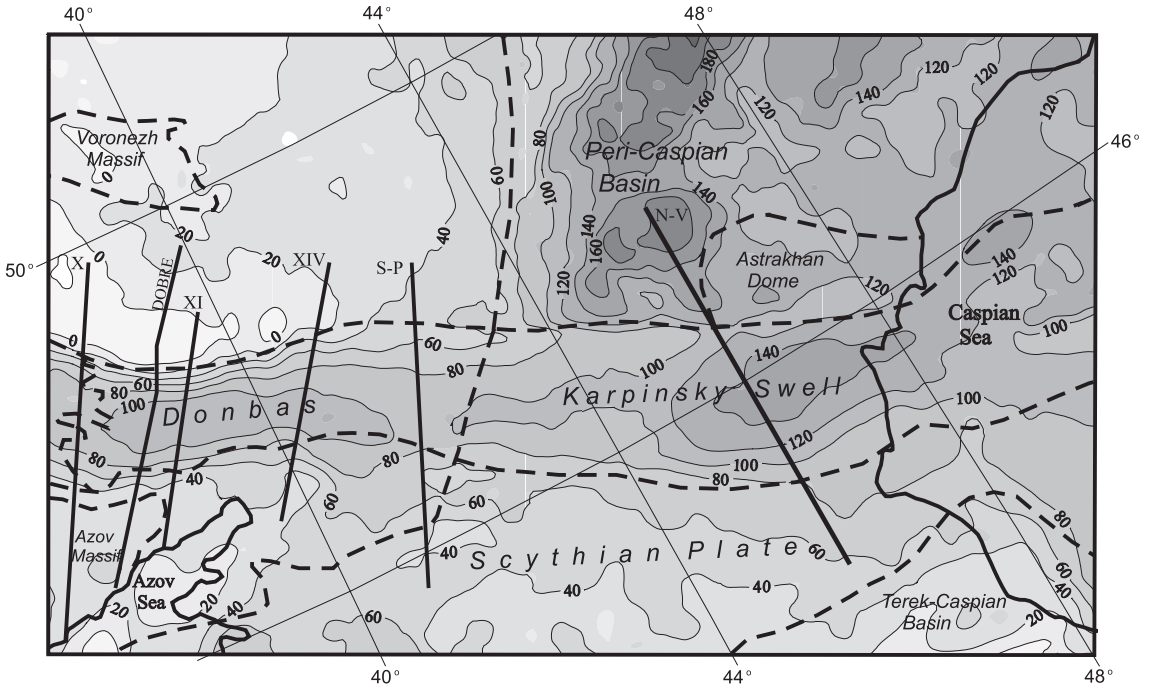

Fig. 9. Residual gravity field of the study area obtained by subtracting the total gravity effect of the two supracrustal model layers (Fig. 7) from the observed gravity field (Fig. 2). Contour interval is 20 mGal. Dashed lines outline tectonic units; solid lines indicate DSS profiles.

ment of the profile (as seen in the figures) where it crosses the KS from the SP to the PCB. It is the first time that these data were modelled using modern, computer-based (ray-tracing) methods that allowed taking into account travel times from all shot points for different types of seismic waves simultaneously.

Continuous seismic profiling was carried out along the Nakhichevan–Volgograd profile with receivers placed every 100 m recording nine shot points from 35 to 65 km apart. Maximum offsets were in the range 200–350 km depending on direction and shotpoint. Recorded seismic phases included those refracted in the sedimentary cover (Ps), reflected (PcP) and refracted (Pg) from the basement (upper and middle crust), reflected (PmP) and refracted (Pn) in the lower crust with apparent velocities 7.5–7.7 kms^{-1}; and reflected (PmP′) and refracted (Pn) from the Moho and within the upper mantle. Note that the phase identification, which follows Baranova and Pavlenkova (2003), is not conventional with Pn referring to lower crustal as well as upper mantle refractions, and PmP and PmP′ being phases reflected from above and below a very high velocity layer defined as lower crust.

The travel times of some of the identified phases for one shot point are plotted in Fig. 10. There are two distinct first-arrival branches with a cross-over distance of about 130–150 km. The first branch has velocities from 2.5–4.0 kms^{-1} to 6.0–6.8 kms^{-1} and corresponds to refracted Ps and Pg phases from

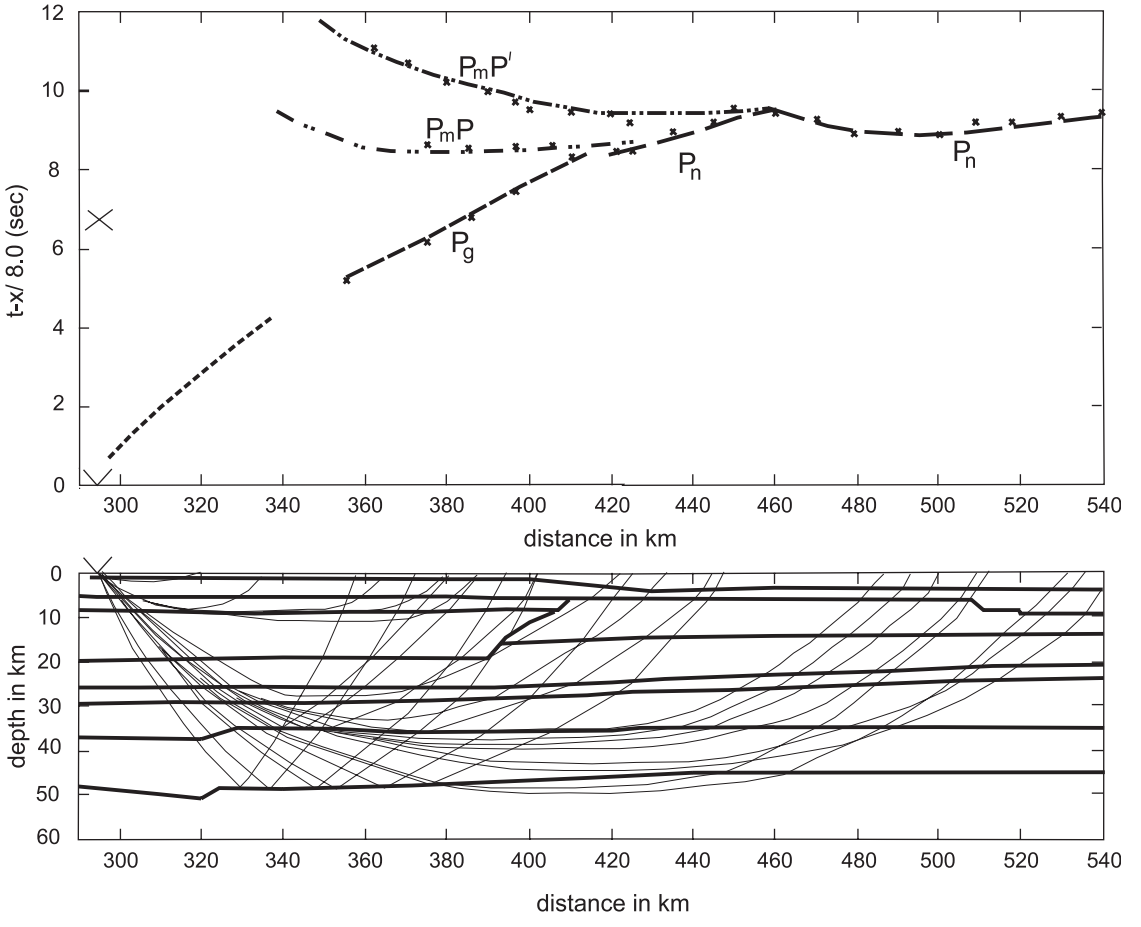

Fig. 10. Observed (crosses) and calculated (lines) travel times, and selected model ray paths, for seismic phases observed on the Nakhichevan–Volgograd DSS profile, shotpoint 4.

the upper and middle parts of the cross-section. The second brach with velocties ≥ 7.5 kms^{-1} is formed by "Pn" arrivals from the lower crust and upper mantle. A more detailed discussion of the travel time data can be found in Baranova and Pavlenkova (2003).

The velocity model determined by Baranova and Pavlenkova (2003) along the Nakhichevan–Volgograd profile is reproduced in Fig. 11. It was calculated using the two-dimensional (2D) forward ray-trace modelling program SEIS-83 (Cerveny and Psencik, 1984), matching observed and calculated travel times first for the Ps and Pg phases and, subsequently, for reflected (PmP and PmP′) and refracted (Pn) waves from the lower crust and the Moho. Selected observed and calculated travel time curves for the final velocity model for one shot point (4) are shown in Fig. 10. The resulting model explains the general features of the observed wave field and satisfies the criterion of model simplicity. In general, it reveals a revised crustal structure for the KS–SP area compared with previous models (e.g., Krasnopevtseva, 1984; cf. Fig. 2a of Ershov et al., 1999).

The velocity model presented in Fig. 11 includes what can be considered two deep sedimentary basins (taking velocities < 5.8 kms^{-1} to be representative of sediments), one beneath the KS and one in the southern PCB. In the latter, the sedimentary succession appears to have a thickness of about 14 km. The 4.5 kms^{-1} horizon—which can be taken as probably corresponding to the top of Palaeozoic metamorphosed sediments (i.e., Palaeozoic basement)—rises to about 1 km depth beneath the KS. This differs from the neighbouring SP and the PCB where it deepens to 4–5 km. In contrast, the 6.0–6.2 kms^{-1} velocity horizon—interpreted as top of crystalline basement—abruptly deepens below the KS (forming a 19–20-km-deep trough). As such, the velocity model is consistent with the structure of the KS shown in Fig. 5 as the uplift of the Palaeozoic basement (considered as a "swell") accompanied by a deepening of the crystalline Precambrian basement horizon.

The middle crust of the central and northern parts of the cross-section is characterised by its gradual northward (towards the PCB) increase of average velocity. The 6.4 and 6.8 kms^{-1} isovelocity contours shallow from depths of 26 and 29 km below the KS to 21 and 24 km correspondingly under the PCB.

The most striking feature of the lower crust of the KS is the horizon at depth 35–38 km, giving rise to reflections PmP (Fig. 10) which are higher in amplitude than the subsequent PmP′ phase (Baranova and Pavlenkova, 2003) and the "Pn" refracted phase. This horizon is the top of a ~ 10-km-thick high-velocity (7.5–7.8 kms^{-1}) lower crustal or crust–mantle transition layer, the base of which is interpreted as the Moho. This layer ceases to exist just at the southern margin of the KS at its junction with the SP (Fig. 11), resulting in a sharp 10 km step in Moho. Upper mantle velocity correspondingly increases from 8.0 to 8.2 kms^{-1}.

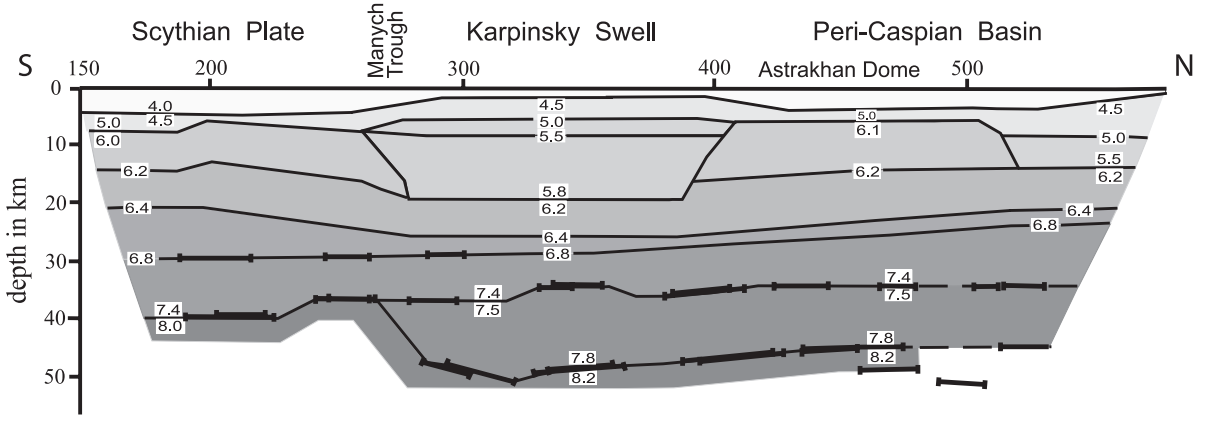

Fig. 11. Velocity model on part of the Nakhichevan–Volgograd DSS profile crossing the Scythian Plate–Karpinsky Swell–Peri-Caspian Basin (thick line labelled NV in previous figures). Velocities are in kms^{-1}. Thick subhorizontal lines indicate reflectors.

According to Baranova and Pavlenkova (2003), the geometry of the 7.5–7.8 kms^{-1} crust–mantle transition body is quite robustly constrained, at least as far north as about km 450–470. Its presence and geometry further northwards, beneath the PCB, are not clear. Earlier studies report that the crust of the PCB is underlain by a high-velocity layer in the uppermost mantle (lying below a refracting Moho boundary with velocity of 8.0–8.1 kms^{-1} (Volozh et al., 1975; Brunet et al., 1999). However, the relationship between this layer and the one seen in Fig. 11 cannot be stated with any certainty.

In any case, there is an abrupt change of crustal and upper mantle geometry between the SP and the KS, and it can be assumed that there are major structures throughout the crust in the narrow, 20–25 km wide, zone lying approximately below the Manych Trough. Such a "fault zone" includes the southern flank of deep sedimentary trough of the KS, the abrupt Moho step, related to the southern edge of the high-velocity crust–mantle layer, and a change in upper mantle seismic velocity.

5.2. Gravity model along the Nakhichevan–Volgograd DSS line

Fig. 12 shows a density cross-section derived from the velocity cross-section in Fig. 11. The densities in the crystalline crust were estimated by using the conversion functions $\rho = 2700 + 270(V_p - 6.0)$ kgm^{-3} for V_p (seismic P-wave velocity) less than 7.0 kms^{-1}, and $\rho = 3020 + 280(V_p - 7.0)$ kgm^{-3} for higher velocities, including the upper mantle (Gordienko, 1999). Densities for the sedimentary succession were determined as before (in the 3D analysis) using laboratory measurements on samples taken from depths up to 6 km, from which appropriate velocity/density conversion functions were determined (Golizdra and Popovich, 1998, 1999). The inferred relationship for the highly compacted and altered sediments of the DF differs from those that are conventionally adopted (e.g., Ludwig et al., 1970; Barton, 1986) with densities being slightly higher for the same velocities.

The density model in Fig. 12, constructed to match the observed gravity data, corresponds closely to the

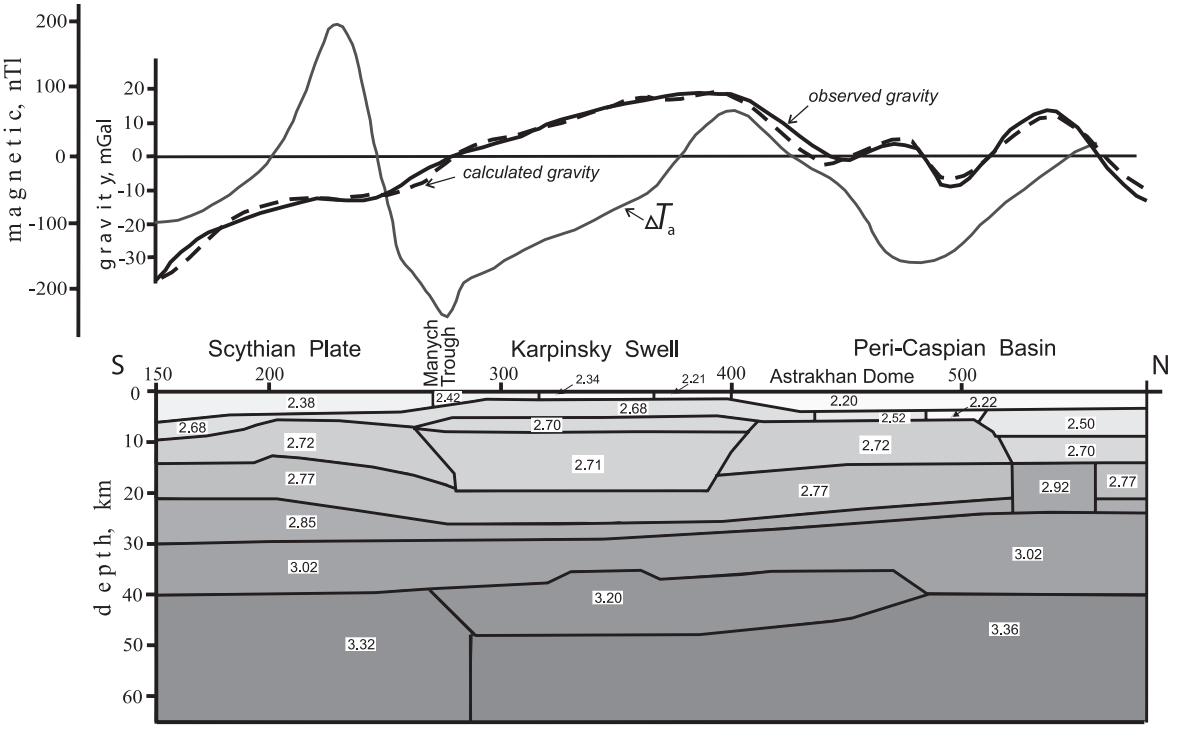

Fig. 12. Density model corresponding to the velocity model shown in Fig. 11. Densities are in 10^{-3} kgm^{-3}.

velocity model in Fig. 11 according to the conversion functions described above. The high-velocity crust–mantle transition layer 40–48 km beneath the KS has a density of 3200 kgm^{-3} which isostatically compensates the mass deficiency effected by 20 km of Palaeozoic rocks with density of 2680–2710 kgm^{-3}, causing the negative residual gravity anomaly (Fig. 8). The gravity model also indicates that the gravity signature of the southern flank of the KS is consistent with the velocity modelling, supporting the presence of a major crustal boundary in this area. Another notable feature is that the Astrakhan Dome, in the southern part of the PCB, is associated with a strong uplift (up to 6 km) of crystalline basement (remnant block of Precambrian basement?) at the junction of the PCB and KS (Fig. 12).

The northern prolongation of the high-density lens beneath the PCB remains unresolved. Otherwise, to explain the character of the observed gravity field in the PCB, a number of small changes in the density model compared to the initial velocity model was introduced. This included a body interpreted as a salt stock with a density of 2200 kgm^{-3} and a base at ~ 8 km to model a gravity low at about km 500 and a body with a density of 2920 kgm^{-3} in the middle crust in the area of local gravity high at km 520. The latter could be related to mafic igneous rocks within the sedimentary succession (cf. Kostyuchenko, 2004).

6. Discussion

3D backstripping of the gravity effect of supracrustal (sedimentary and metasedimentary) successions has revealed that the southern margin of the EEC is characterised by a number of positive residual gravity anomalies. These indicate the presence of crustal and upper mantle heterogeneities, including Moho relief, that are a consequence of the tectonic history of the area, in particular, during the assembly of the crustal units in this area beginning in the late Palaeozoic. There are four main zones of positive residual gravity anomalies: the DF, the western KS, the eastern KS and northern Caspian Sea, and the central PCB. The last two are further elucidated by 2D gravity modelling based on newly reinterpreted DSS data. The four anomalous zones are discussed below in terms of several key tectonic episodes affecting the study area, namely, Middle–Late Devonian rifting, Early Permian effects related to Uralian orogenesis, and Cimmerian (Triassic–Jurassic) and Alpine (Cretaceous–Tertiary) convergence and orogenesis.

6.1. Dniepr-Donets and Peri-Caspian basins

The DF is the uplifted and mildly compressionally deformed southeastern segment of the intracratonic DDB rift basin. Previous investigations (Yegorova et al., 1999) deduced that the DF residual gravity anomaly is caused by the presence of a high-density/velocity body in the crystalline crust beneath the sedimentary depocentre (depths greater than 20 km) emplaced as a result of intrusion of mafic and ultramafic magmas during the main phase of active rifting in the late Palaeozoic. This interpretation is strongly supported by recent refraction/wide-angle seismic (DOBREfraction'99 Working Group, 2003) and deep seismic reflection studies (Maystrenko et al., 2003) in the DF.

Middle–Late Devonian rifting, such as that formed the DDB, was widespread throughout the whole of the EEC (Nikishin et al., 1996). It has been suggested that the thermal and geodynamic evolution of the craton at this time may have been governed by the activity of several mantle plumes (Wilson and Lyashkevich, 1996). Indeed, Chekunov (1994) proposed that one such plume, located under the PCB, could be considered as the "parent" of the DDB. The Late Devonian was clearly also a time of significant extension and subsidence in the PCB (e.g., Brunet et al., 1999). It is generally thought that there was also an earlier—Riphean–Early Palaeozoic—rifting and subsidence phase. Some authors consider that extension was so great that the PCB is underlain by Devonian-aged oceanic crust (Zonenshain et al., 1990; Kostyuchenko et al., 1999). Others consider that Precambrian continental crust, severely attenuated and intruded by mafic magmas during Devonian rifting, underlies in the PCB (e.g., Belousov, 1990). Existing interpretations of DSS data collected in the PCB indicate that there is no "granitic" layer in the crust and that sediments lie directly upon crust of velocity 6.8–7.2 kms^{-1} (Kostyuchenko et al., 1999). There are also localised high-velocity lower crustal lenses that correlate with gravity maxima (Volozh et al., 1975).

The 160–180 mGal residual gravity anomaly that characterises the central PCB could be, by analogy with the DF, the signature of high-density (lower) crustal bodies related to mantle intrusion during Middle–Late Devonian rifting. If, indeed, the DF and PCB residual anomalies have a similar nature and common origin, then the DDB–DF and the PCB could be considered as two branches of the same Middle–Late Devonian rift system, as proposed by Zonenshain et al. (1990). According to Zonenshain et al. (1990), the DDB is a "failed arm" of a former triple junction of rifts with one of the two "successful" arms leading to the generation of oceanic crust beneath the PCB. The other arm presumably passed southwards from a junction of the DF with the PCB (i.e., the junction of the DF, KS, and the PCB in Fig. 9 and others). As such, the Astrakhan Dome, situated in the southwestern part of the PCB near its junction with the KS and clearly seen in Figs. 11 and 12 as an uplift of the crystalline basement, may be considered as a remnant block separated from the EEC by Devonian rifting on the central axis of the PCB.

The southern margin of the EEC was a passive margin until at least the end of the early Carboniferous (Nikishin et al., 1996; cf. Golonka, 2004). In the Early Permian, the Urals Orogeny culminated and the eastern and southeastern margins of the EEC were, accordingly, affected by this. The PCB at this time was blocked from the south by the northwards emplacement of the continental Usturt Massif, resulting in its isolation from the open sea and conversion into a salt-bearing basin (Zonenshain et al., 1990). The positive residual gravity field of the eastern KS and under the northern Caspian Sea (with anomalies regionally greater than 140 mGal) is possibly a signature of these events. As such, the southernmost and southeasternmost parts of the PCB constitute a folded and thrusted zone formed at this time, confined to the south by the South Emba Uplift (Zonenshain et al., 1990). The gravitational signature of this, as seen in the residual anomaly map (Fig. 9), is likely caused by a density increase within the crystalline crust (and subcrustal lithosphere?) combined with increased densities of sediments that have been involved in the folding and thrusting deformation. Similar features can be seen in the southern Urals (e.g., Zalair Formation; Khain, 1977).

6.2. Karpinsky Swell and Scythian Plate

The residual gravity high over the western part of the KS (Fig. 9) can be explained by higher than average densities within the crystalline crust compared to those of the neighbouring SP. Heterogeneities within the lithosphere along the southern margin of the EEC in this region can be generally ascribed to Mesozoic–Cainozoic events taking place in mainly compressional or transpressional tectonic setting (cf. Golonka, 2004, this volume). The KS residual anomaly and its causes are, as such, not dissimilar to what has been inferred for the western boundary of the EEC in the vicinity of the Trans-European Suture Zone (TESZ) in Poland and environs (Yegorova and Starostenko, 1999). The latter has been interpreted as related to the complex evolution of the collision–accretion zone between Phanerozoic Western Europe and the Precambrian EEC since the Late Proterozoic (Yegorova and Starostenko, 1999).

The Mesozoic–Cainozoic development of the KS was dominated by Cimmerian (Late Triassic–Early Jurassic) and Alpine (Cretaceous–Tertiary) compressional phases related to orogenesis in the Caucasus (Zonenshain et al., 1990; Sobornov, 1995) located some 300 km to the south (Fig. 1). Sobornov (1995) argued on the basis of seismic reflection data that the age of the main phase of thrusting (and "inversion") of the KS was Cimmerian. A second, Alpine, episode is recognised along the southern flank of the KS (Sobornov, 1995). Stovba and Stephenson (1999), from seismic data, and Saintot et al. (2003), from structural mapping, argue that the compressional deformation forming the DF occurred at these times as well, especially the Alpine. Thus, the structural inversion of the KS (and probably the DF) appears to be related mainly to stresses developed in the Caucasus collisional zone and transmitted some 300 km through the SP (i.e., Zonenshain et al., 1990; Sobornov, 1995).

The reinterpreted Nakhichevan–Volgograd DSS profile, supported by gravity modelling, indicates an abrupt tectonic zone penetrating the entire crust on the southern border of the KS (Fig. 12). This zone also has a significant magnetic character (Figs. 3 and 12) and coincides with the Manych Trough, expressed in recent times by a system of rivers and lakes. The abrupt plunge of the Moho from 40 km below the SP to 48 km below the KS corresponds with the appearance of a 10-km-thick high-velocity (7.5–7.8 kms^{-1}) layer in

the lower crust (or crust–mantle transition layer). The correspondingly high-density (3200 kgm^{-3}) of this layer essentially compensates the 20-km-thick sedimentary succession of the KS, whose gravity effect removed from the Bouguer field gives the positive residual anomaly seen in Fig. 9. Such heterogeneities may be typical for lower crust formed convergence zones. For example, a very similar high-velocity lower crustal layer is recognised in the Urals (Druzhinin et al., 1997). A high-velocity (7.5–7.7 kms^{-1}) lens at the base of the crust together with an upper mantle reflector is also seen on the EUROBRIDGE-97 profile over the Early Proterozoic-aged Fennoscandia/Sarmatia suture zone within the EEC (e.g., Yegorova et al., 2004).

The inferred crustal structure of the KS, with its high-velocity/density layer, is also likely a consequence of accretionary processes, the same as those expressed by folding and thrusting near the surface of the KS. The abrupt crustal boundary between the SP and the KS implies a convergence between the SP and EEC, with the KS being an element of the resulting accretionary zone. The age of thrusting on the KS (Sobornov, 1995) shows that this is of Mesozoic and younger age.

Also noteworthy is that the crustal structure of the KS, at least where it is crossed by the Nakhichevan–Volgograd profile, is distinctly different from that of the DF. There is no comparable deepening of the Moho, associated with a high-velocity crust–mantle mix layer, under the latter, although there is a rift "pillow" in the lower crust introduced by mafic intrusion during rifting in the late Palaeozoic (DOBREfraction'99 Working Group, 2003).

7. Summary and conclusions

The southern margin of the EEC is characterised by a complex crustal structure derived from its complex tectonic history which included a variety of extensional and convergent tectonic processes. Available geological and seismic information for the area was used to compile two structure maps, one at the base of Mesozoic–Cainozoic sediments (top of Palaeozoic successions) and the other at the top of the crystalline Precambrian basement. These maps have served as a basis for a 3D gravity analysis of the crust of the study area, beginning with the computation of a residual gravity field from which the gravity effects of supracrustal sedimentary successions have been removed.

The residual gravity field is characterised by a NW–SE elongated zone of positive residual anomalies along the southern margin of the EEC, from the DF through the KS to the northern part of the Caspian Sea (southern part of the PCB), and a positive anomaly along the central axis of the PCB. The density heterogeneities in the lithosphere signified by these residual anomalies are assumed to have formed as the result of first-order tectonic processes affecting the southern margin of the EEC since the late Palaeozoic. These include late Palaeozoic (Middle–Late Devonian) rifting in the DF and central PCB, the Early Permian Urals Orogeny affecting the southern margin of the PCB and, possibly, eastern KS, and orogenesis in the Caucasus and associated Cimmerian and Alpine convergence tectonics between the SP and KS (and eastern DF).

2D gravity modelling constrained by a new interpretation of DSS data along the Nakhichevan–Volgograd DSS profile, which crosses the central KS, shows that the southern border of the KS corresponds to a major crustal penetrating tectonic zone coinciding at the surface with the Manych Trough. This zone divides the crust into two distinct structural segments, one associated with the SP to the south and the other with the KS and adjacent PCB. A diagnostic feature of the lower crust of the KS is a crust–mantle transition zone in the depth range 40–48 km with velocity of 7.5–7.7 kms^{-1} and density of 3200 kgm^{-3}, a feature not found beneath the DF. This suggests that the KS might not be considered as a prolongation of the DDB–DF intracratonic rift zone. More likely, the KS is an element of the transition zone formed along the southern margin of the EEC by accretion of the SP to the EEC in Mesozoic–Cainozoic times.

Acknowledgements

The scientific investigations leading to this paper were undertaken as part of INTAS project 97-0743, coordinated by R. Stephenson, and in the framework of the European Science Foundation EUROPROBE GeoRift project. We extend our appreciation to N.I. Pavlenkova (Institute of Physics of the Earth, Russian Academy of Sciences) for providing the initial DSS data for reinterpretation, assistance, and comments,

and to V.G. Kozlenko (Institute of Geophysics, Kiev) for fruitful discussions on the interpretation. M.F. Brunet (University of Pierre and Marie Curie, Paris) and V.O. Mikhailov (Institute of Physics of the Earth, Russian Academy of Sciences) are thanked for their critical reviews and helpful comments on the paper.

References

Aizberg, R.E., Garetskij, R.G., Sinichka, A.M., 1971. Sarmatsko–Turanian lineament of the earth's crust (in Russian). In: Peive, A.V. (Ed.), Problems of Theoretical and Regional Tectonics. Nauka, Moscow, pp. 41–51.

Artemjev, M.E., 1975. Isostasy of the Territory of the USSR. Nauka, Moscow (in Russian).

Artemjev, M.E., Kaban, M.K., Kucherinenko, V.A., Demyanov, G.V., Taranov, V.A., 1994. Subcrustal density inhomogeneities of Northern Eyrasia as derived from the gravity data and isostatic models of the lithosphere. Tectonophysics 240, 249–280.

Atlas of Geological Structure and Oil and Gas Resources of the Dnieper–Donets Basin, 1984. Ministry of Geology of the Ukrainian SSR. Ukrainian Scientific Research Institute of Geological Prospecting, Kiev 190 pp. (in Russian).

Baranova, E.P., Pavlenkova, N.I., 2003. Structure of the lower crust below the Karpinsky Swell. Izvestia. Physics of the Solid Earth 6, 76–84.

Barton, P.J., 1986. The relationships between seismic velocity and density in the continental crust—a useful constraint? Geophysical Journal of the Royal Astronomical Society 87, 195–208.

Belousov, V.V., 1990. Tectonosphere of the earth: upper mantle and crust interaction. Tectonophysics 180, 139–183.

Bogdanov, A.A., Khain, V.E., 1981. International Tectonic Map of Europe and Adjacent Regions, 1:2,500,000 scale. Academy of Sciences of the USSR, Moscow, UNESCO.

Borodulin, M.A., 1973. Methodics of the investigations and structure of the Earth's crust along the DSS profile Bataisk–Milutinskaya (Donbas). Geophysical Sbornik 6, 20–28 (in Russian).

Brunet, M.-F., Volozh, Yu.A., Antipov, M.P., Lobkovsky, L.I., 1999. The geodynamic evolution of the Precaspian Basin (Kazakhstan) along a north–south section. Tectonophysics 313, 85–106.

Cerveny, V., Psencik, I., 1984. SEIS-83—numerical modelling of seismic wave field in 2-D laterally varying layered structures by the ray method. In: Engdahl, E.R. (Ed.), Documentation of Earthquake Algorithm Word Data Center (A) for Solid Earth Geophysics. Boulder, CO, Paper SE-35, 36–40.

Chekunov, A.V., 1994. To geodynamics of the Dnieper-Donets rift-geosyncline. Geophysical Journal (Kiev) 3 (v. 16), 3–13 (in Russian).

Chekunov, A.V., Gavrish, V.K., Kutas, R.I., Ryabchum, L.I., 1992. Dnieper-Donets palaeorift. Tectonophysics 208, 257–272.

Christensen, N.I., Mooney, W.D., 1995. Seismic velocity structure and composition of the continental crust: a global view. Journal of Geophysical Research 100, 9761–9789.

DOBREfraction'99 Working Group, 2003. DOBREFraction'99—velocity model of the crust and upper mantle beneath the Donbas Foldbelt (East Ukraine). Tectonophysics 371, 81–110.

Dobrohotov, M.N., 1961. Geology of the Precambrian of the KMA (Kursk magnetic anomalies). Soviet Geology 11, 33–54 (in Russian).

Druzhinin, V.S., Kashubin, S.N., Kashubina, T.V., et al., 1997. The main features of the interface between the crust and upper mantle in the Middle Urals (in the vicinity of the deep drillhole SG-4). Tectonophysics 269, 259–267.

Ershov, A.V., Brunet, M.-F., Korotaev, M.V., Nikishin, A.M., Bolotov, S.N., 1999. Late Cenozoic burial history and dynamic of the Northern Caucasus molasse basin: implications for foreland basin modelling. Tectonophysics 313, 219–241.

Golizdra, G.Ya., Popovich, V.S., 1998. Density models of the sedimentary succession of the south-eastern part of the DDB, western and northern margins of the Donbas. Geophysical Journal (Kiev) 6 (v. 20), 117–123 (in Russian).

Golizdra, G.Ya., Popovich, V.S., 1999. The velocity–density relation of the rocks of the sedimentary succession of the south-eastern part of the Dnieper-Donets Basin. Geophysical Journal (Kiev) 5 (v. 21), 72–75 (in Russian).

Golonka, J., 2004. Plate tectonic evolution of the southern margin of Eurasia in the Mesozoic and Cenozoic. Tectonophysics, 381, 235–273 (this volume).

Gordienko, V.V., 1999. Density Models of the Tectonosphere of the Territory of the Ukraine. Intellect, Kiev (in Russian).

Ilchenko, T., 1996. Dnieper-Donets Rift: deep structure and evolution from DSS profilling. Tectonophysics 268, 83–98.

Ilchenko, T.V., Stepanenko, V.M., 1998. The velocity model of the Earth's crust and uppermost mantle below the Donbas and its geological interpretation. Geophysical Journal (Kiev) 2 (v. 20), 95–104 (in Russian).

Karpinskii, A.P., 1883. The remarks on the character of dislocations of rocks in the southern part of European Russia. Mining Journal III, 45–55 (in Russian).

Khain, V.E., 1977. Regional Geotectonics. Extra-Alpine Europe and Western Asia. Nedra, Moscow (in Russian).

Konovaltcev, Yu.P., 1978. Revealing the fault zones on refracted waves along the DSS-CDP profile Peschanokopskoe–Surovikino. Razvedochnaya Geofizika 82, 104–108 (in Russian).

Kostyuchenko, S.L., Egorkin, A.V., Solodolov, L.N., 1999. Structure and genetic mechanisms of the Precambrian rifts of the East-European platform in Russia by integrated study of seismic, gravity and magnetic data. Tectonophysics 313, 9–28.

Kostyuchenko, S.L., Morozov, A.F., Stephenson, R.A., Solodilov, L.N., Vedrentsev, A.G., Popolitov, K.E., Aleshina, A.F., Vishnevskaya, V.S., Yegorova, T.P., 2004. The evolution of the southern margin of the East European Craton based on seismic and potential field data. Tectonophysics, 381, 101–118 (this volume).

Kozlenko, V.G., 1986. The basis of construction of regional seismic and gravity models (in Russian). In: Magnitskij, V.A., Sollogub, V.B., Starostenko, V.I. (Eds.), Studying the Lithosphere by Geophysical Methods. Naukova Dumka, Kiev, pp. 113–122.

Krasnopevtseva, G.V., 1984. Deep Structure of Caucasus Seismoactive Region. Nauka, Moscow (in Russian).

Kusznir, N.J., Stovba, S.M., Stephenson, R.A., Poplavskii, K.N.,

1996. The formation of the northwest Dnieper-Donets Basin: 2-D forward and reverse syn-rift and post-rift modelling. Tectonophysics 268, 237–255.

Kutas, R.I., Pashkevich, I.K., 2000. Geothermal and magnetic models of the Earth's crust of Donbas (joint tectonic analysis with the DSS data). Geophysical Journal (Kiev) 4 (v. 22), 21–36 (in Russian).

Ludwig, J.W., Nafe, J.E., Drake, C.L., 1970. Seismic refraction. In: Maxwell, A.E. (Ed.), The Sea, vol. 4. Wiley, New York, pp. 55–84.

Maystrenko, Yu., Stovba, S.M., Stephenson, R.A., Bayer, U., Menyoli, E., Gajewski, D., Huebscher, C., Rabbel, W., Saintot, A., Starostenko, V., Thybo, H., Tolkunov, A., 2003. Crustal-scale pop-up structure in cratonic lithosphere: DOBRE deep seismic reflection study of the Donbas Foldbelt, Ukraine. Geology 31 (8), 733–736.

McCann, T. et al., 2003. Geological Society of London. Special Publication.

Milanovsky, E.E., 1987. Geology of the USSR. Moscow University Press, Moscow (in Russian).

Milanovsky, E.E., 1992. Aulacogens and aulacogeosynclines: regularities in setting and evolution. Tectonophysics 215, 55–68.

Muratov, M.V. (Ed.), 1975. Map of Deep Structure of Azov-Caspian Region, 1:500,000 scale, 1975. Moscow Geological Institute, Moscow.

Nazarevich, B.P., Nazarevich, I.A., Shvudko, N.I., 1986. Nogaiskaya (Upper Triassic) volcanic-sedimentary formation of the Eastern Fore–Caucasus—the composition and relationships with pre- and post-Nogaisk volcanic rocks (in Russian). Formations of the Sedimentary Basins. Nauka, Moscow, pp. 67–86.

Nevolin, N.V., Kunin, N.Ya., 1977. Geological Structure and Oil and Gas Perspectives of Salt Dome Basins of Continents According to Geophysical Data. Nedra, Moscow (in Russian).

Nikishin, A.M., Ziegler, P.A., Stephenson, R.A., Cloetigh, S.A.P.L., Furne, A.V., Fokin, P.A., Ershov, A.V., Bolotov, A.V., Korotaev, M.V., Alekseev, A.S., Gorbachev, V.I., Shipilov, E.V., Lankreijer, A., Bembinova, E.Yu., Shalimov, I.V., 1996. Late Precambrian to Triassic history of the East European Craton: dynamics of sedimentary basin evolution. Tectonophysics 268, 23–63.

Ozerskaya, M.L., Podoba, N.V., 1967. Physical Properties of the Sedimentary Cover of the Territory of the USSR. Nedra, Moscow (in Russian).

Pavlenkova, N.I., 1995. Double moho in the Dnieper-Donets Basin. Compte-Rendu. Acad. Science. Paris 321 (Ser. IIa), 85–93.

Saintot, A., Stephenson, R., Brem, A., Stovba, S., Privalov, V., 2003. Paleostress field reconstruction and revised tectonic history of the Donbas fold and thrust belt (Ukraine and Russia). Tectonics 22 (5), 1059. doi:10.1029/2002TC001366,2003

Simonenko, T.N., Pashkevich, I.K. (Ed.), 1990. Map of Anomalous Magnetic Field of Europe, scale 1:5,000,000. Mining Institute, Leningrad.

Sobornov, K., 1995. Structural evolution of the Karpinsky Swell, Russia. Compte-Rendu. Acad. Science, Pariss 321 (Ser. IIa), 161–169.

Starostenko, V.I., Legostaeva, O.V., 1998. Direct gravity problem for heterogeneous arbitrary truncated vertical rectangular prism. Izvestia. Physics of the Solid Earth 12, 31–44.

Starostenko, V.I., Matsello, V.V., Aksak, I.N., Kulesh, V.A., Legostaeva, O.V., Yegorova, T.P., 1997. Automated input into computer the images of geophysical maps and construction of their digital models. Geophysical Journal (Kiev) 1 (v. 19), 3–13 (in Russian).

Stephenson, R.A., Stovba, S., Starostenko, V.I., 2001. Pripyat–Dnieper-Donets Basin: implications for dynamics of rifting and the tectonic history of the northern Pery-Tethys platform. In: Ziegler, P.A., Cavazza, W., Robertson, A.H.F. (Eds.), Peri-Tethys Memoir 6, "Peri-Tethian Rift–Wrench Basins and Passive Margins". Memoires du Museum Natioanal d'Histoire Naturelle 186, 369–406.

Stovba, S., Stephenson, R.A., Kivshik, U., 1996. Structural features and evolution of the Dnieper-Donats Basin, Ukraine, from regional seismic reflection profiles. Tectonophysics 268, 127–147.

Stovba, S.N., Stephenson, R.A., 1999. The Donbas foldbelt: its relationships with the uninverted Donets segment of the Dniepr-Donets Basin, Ukraine. Tectonophysics 313, 59–83.

Thybo, H., Pharaoh, T., Guterh, A. (Eds.), 1999. Geophysical Investigations of the Trans-European Suture Zone. Tectonophysics vol. 314. Special issue, 350 pp.

Volozh, Yu.A., Sapozhnikov, R.B., Tsimmer, V.A., 1975. Structure of the crust in the Caspian depression. International Geology Review 19, 25–33.

Wilson, M., Lyashkevich, Z.M., 1996. Magmatism and the geodynamics of the Pripyat–Dnieper-Donets rift, East European platform. Tectonophysics 268, 65–81.

Yegorova, T.P., 2000. Three-dimensional modelling of earth's crust structure of the Dnieper-Donets Basin and Donbas: I. Sedimentary strata. Geophysical Journal (Kiev) 5 (v. 22), 109–119 (in Russian).

Yegorova, T.P., Starostenko, V.I., 1999. Large-scale three-dimensional gravity analysis of the lithosphere below the transition zone from western Europe to the East European Platform. Tectonophysics 314, 83–100.

Yegorova, T.P., Kozlenko, V.G., Pavlenkova, N.I., Starostenko, V.I., 1995. 3-D density model for the lithosphere of Europe: construction method and preliminary results. Geophysical Journal International 121, 873–892.

Yegorova, T.P., Starostenko, V.I., Kozlenko, V.I., Pavlenkova, N.I., 1998. Three-dimensional gravity modelling of the European Mediterranean lithosphere. Geophysical Journal International 129, 355–367.

Yegorova, T.P., Stephenson, R.A., Kozlenko, V.G., Starostenko, V.I., Legostaeva, O.V., 1999. 3-D gravity analysis of the Dnieper-Donets Basin and Donbas Foldbelt, Ukraine. Tectonophysics 313, 41–58.

Yegorova, T.P., Starostenko, V.I., Kozlenko, V.I., Yliniemi, Yu., 2004. Lithosphere structure of the Ukrainian Shield and Pripyat Trough in the region of EUROBRIDGE-97, Ukraine and Belarus, from gravity modelling data. Tectonophysics, 381, 29–59 (this volume).

Zonenshain, L.P., Kuzmin, M.I., Natapov, L.M., 1990. Geology of the USSR: a plate-tectonic synthesis. American Geophysical Union, Geodynamic Series 21.